FOXL2 Interacts with Steroidogenic Factor-1 (SF-1) and Represses SF-1-Induced *CYP17* Transcription in Granulosa Cells

Mira Park,* Eunkyoung Shin,* Miae Won, Jae-Hong Kim, Hayoung Go, Hyun-Lee Kim, Jeong-Jae Ko, Kangseok Lee, and Jeehyeon Bae

Department of Biomedical Science (M.P., M.W., J.-H.K., H.-L.K., J.-J.K., J.B.), College of Life Science, CHA University, Seongnam 463-836, Korea; and Department of Life Science (E.S., H.G., K.L.), Chung-Ang University, Seoul 156-756, Korea

Mutations in *FOXL2* are responsible for blepharophimosis-ptosis-epicanthus inversus syndrome (BPES) type I, in which affected women exhibit premature ovarian failure. FOXL2-null mice showed defects in granulosa cell development during folliculogenesis. We screened a rat ovarian yeast two-hybrid cDNA library to identify FOXL2-interacting proteins and found steroidogenic factor-1 (SF-1). Here, we show that human FOXL2 and SF-1 proteins interact in human granulosa cells and that FOXL2 negatively regulates the transcriptional activation of a steroidogenic enzyme, CYP17, by SF-1. Furthermore, FOXL2 mutants found in blepharophimosis-ptosis-epicanthus inversus syndrome type I patients lost the ability to repress *CYP17* induction mediated by SF-1. Chromatin immunoprecipitation and EMSA results further revealed that FOXL2 inhibited the binding of SF-1 to the *CYP17* promoter, whereas the FOXL2 mutants failed to block this interaction. Therefore, this study identifies a novel regulatory role for FOXL2 on a key steroidogenic enzyme and provides a possible mechanism by which mutations in FOXL2 disrupt normal ovarian follicle development. **(*Molecular Endocrinology* 24: 1024–1036, 2010)**

FOXL2 is a winged-helix/forkhead (FH) domain transcription factor, and mutations in the *FOXL2* gene are responsible for blepharophimosis-ptosis-epicanthus inversus syndrome (BPES) (OMIM no. 110100) type I, in which affected women exhibit premature ovarian failure (POF) (1). *In situ* hybridization and immunohistochemistry studies confirm that FOXL2 is mainly localized to undifferentiated granulosa cells in the ovary (2, 3). In $FoxL2^{lacZ}$ homozygous mutant murine ovaries, failure of granulosa cell differentiation leads to premature activation of primordial follicles and consequent follicular depletion and atresia (4). Earlier reports indicated that disruption of FOXL2 in mice leads to a block in ovarian follicle development due to the failure of somatic cell development around growing oocytes (3). Thus, unveiling the downstream targets of FOXL2 would greatly enhance our understanding of ovarian physiology and pathology.

In an effort to understand the signaling pathway of FOXL2, we screened a rat ovarian cDNA library to identify FOXL2-interacting proteins using the yeast two-hybrid system and found steroidogenic factor-1 (SF-1). The Nagahama group (5) also recently reported the *in vitro* association of tilapia fish SF-1 with FoxL2. SF-1 is an orphan nuclear hormone receptor, also known as NR5A1 and Ad4BP, and is essential for gonadal development, because SF-1-mutant mutant mice lack gonadotropes in the pituitary (6). In the rodent ovary, SF-1 is widely expressed in the nucleus of granulosa, theca, and interstitial cells (7). SF-1 is a transcription factor that binds

ISSN Print 0888-8809 ISSN Online 1944-9917
Printed in U.S.A.

doi: 10.1210/me.2009-0375 Received September 14, 2009. Accepted January 27, 2010.
First Published Online March 5, 2010
* M.P. and E.S. contributed equally to this work.

Abbreviations: Ala, Alanine; BPES, blepharophimosis-ptosis-epicanthus inversus syndrome; ChIP, chromatin immunoprecipitation; DAPI, 4′,6-diamidino-2-phenylindole; DBD, DNA-binding domain; DTT, dithiothreitol; FBS, fetal bovine serum; FH, forkhead; GAPDH, glyceraldehyde-3-phosphate dehydrogenase; HA, hemagglutinin; LBD, ligand-binding domain; LRH, liver receptor homolog; NP-40, Nonidet P-40; PBS-T, PBS containing 0.01% Tween 20; POF, premature ovarian failure; SDS, sodium dodecyl sulfate; siRNA, small interfering RNA; SF-1, steroidogenic factor-1; WT, wild type.

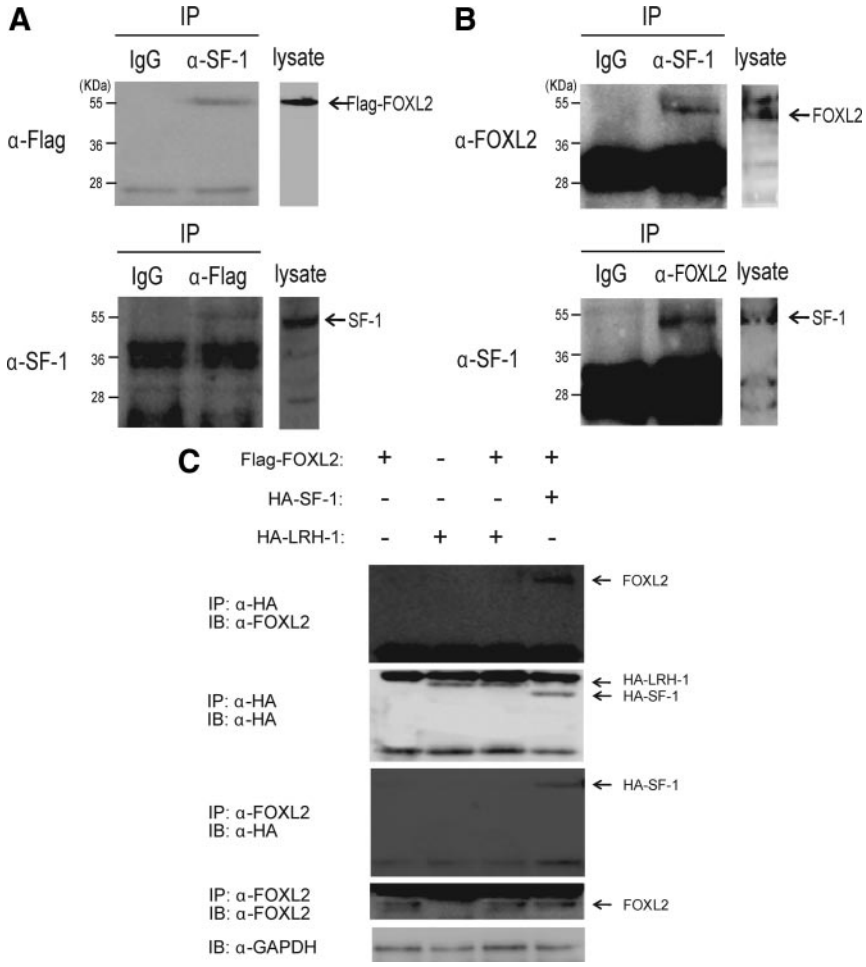

FIG. 1. *In vivo* association of FOXL2 with SF-1. A, Flag-FOXL2 and SF-1 proteins were overexpressed in 293T cells for 24 h. The cell lysates were immunoprecipitated with either α-SF-1 or α-Flag M2 antibodies and subjected to Western blot analyses using α-Flag M2 or α-SF-1, respectively. B, The interaction of endogenous FOXL2 and SF-1 proteins in KGN cells was also confirmed by immunoprecipitation using α-FOXL2 and α-SF-1 antibodies. C, After overexpression of Flag-FOXL2, HA-SF-1, and HA-LRH-1 proteins in 293T cells, the cell lysates were immunoprecipitated (IP) and Western blotted (immunoblot, IB) with either α-HA or α-FOXL2 antibodies.

to the promoters of steroidogenic enzymes, including CYP11A, CYP17, CYP19, and StAR, and regulates their expression (8).

Here, we found that endogenous FOXL2 and SF-1 proteins interact in a human granulosa cell line, and that FOXL2 negatively regulates the transcriptional activity of SF-1 on the steroidogenic enzyme, CYP17. Interestingly, the FOXL2 mutants identified in POF patients with BPES type I failed to repress SF-1-mediated *CYP17* gene induction. Chromatin immunoprecipitation (ChIP) and EMSA results revealed that wild-type (WT) FOXL2 inhibited the interaction of SF-1 with the *CYP17* promoter, whereas mutant FOXL2 failed to block the association of SF-1 with the *CYP17* promoter. Therefore, this study identifies a novel regulatory role for FOXL2 and provides a possible mechanism by which mutations in FOXL2 disrupt normal ovarian follicle development.

Results

Interaction of FOXL2 with SF-1

The *in vivo* interaction between the FOXL2 and SF-1 proteins was demonstrated by immunoprecipitation using anti-SF-1 or anti-Flag M2 antibodies after overexpression of Flag-tagged FOXL2 and Flag-tagged SF-1 in 293T cells (Fig. 1A). In addition, association of endogenously expressed FOXL2 and SF-1 proteins in the human granulose cell line KGN (10) was confirmed by coimmunoprecipitation (Fig. 1B). Because liver receptor homolog (LRH)-1 (NR5A2) is a member of the nuclear receptor NR5A subfamily as is SF-1 (NR5A1), we examined the binding activity of FOXL2 to LRH-1 in 293T cells. In contrast to SF-1, LRH-1 did not associate with FOXL2 based on the immunoprecipitation experiments (Fig. 1C), suggesting a specific interaction between FOXL2 and SF-1.

Identification of the domain involved in the interaction between FOXL2 and SF-1

To identify the domain of SF-1 that is involved in the association with FOXL2, DNA constructs that code for partially truncated mutants of SF-1 were generated (Fig. 2A) and their binding capacity for FOXL2 was analyzed by immunoprecipitation after their overexpression. SF-1 is a 461-amino acid protein with two zinc finger DNA-binding domains (DBDs) and a ligand-binding domain (LBD) separated by a hinge (Fig. 2A). Mutant SF-1 with a complete (1-240) or a partial loss (1-350) of the LBD efficiently formed a complex with FOXL2 (Fig. 2B). In contrast, a SF-1 mutant with a truncated N terminus, leading to the loss of the DBD and the hinge region (220-461), lost its interaction with FOXL2 (Fig. 2B). Furthermore, the binding of FOXL2 was abolished by a minimal deletion of the DBD from SF-1 (90-461) (Fig. 2B), suggesting that the DBD of SF-1 plays a critical role in its association with FOXL2, whereas other regions, including the hinge and the LBD of SF-1, do not.

Inhibitory effect of FOXL2 on SF-1-mediated CYP17 transcriptional activation

Ectopic expression of SF-1 greatly transactivated the *CYP17* promoter in KGN cells by over 100-fold (Fig. 3A). However, coexpression with full-length FOXL2 nearly

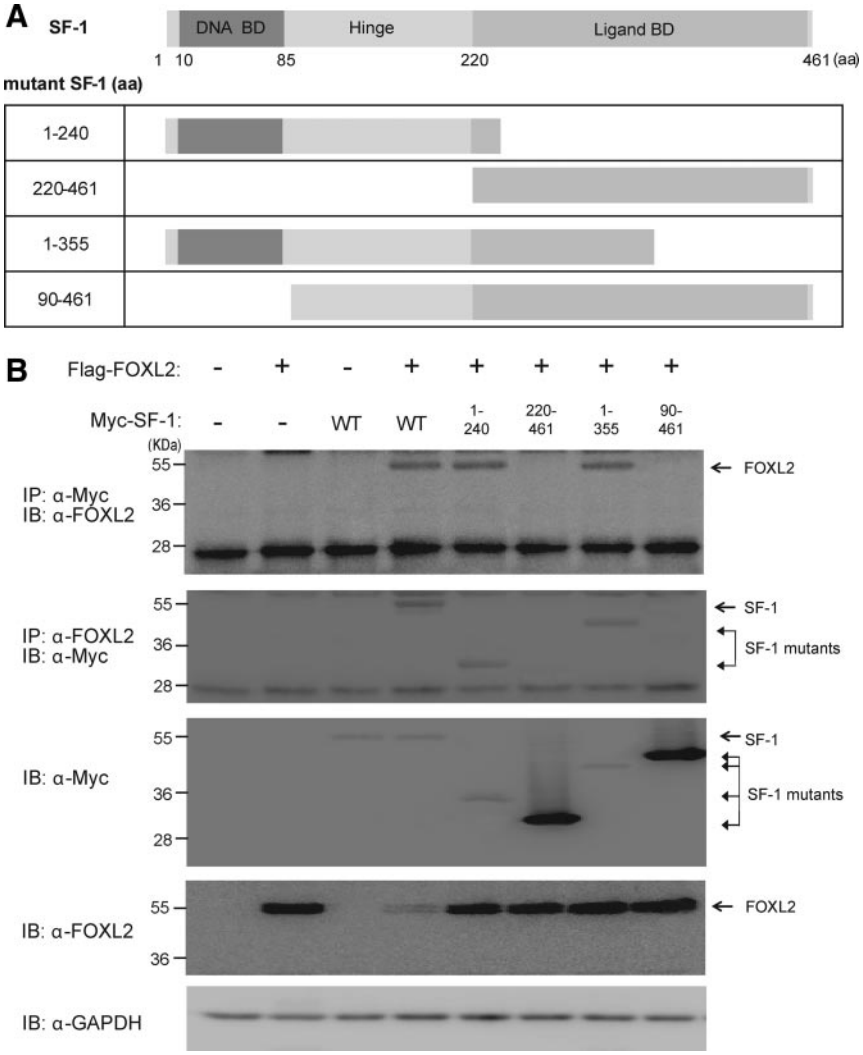

FIG. 2. Identification of the domain of SF-1 involved in binding with FOXL2. A, Secondary structures of WT SF-1 containing the DBD, hinge region, and LBD, and truncated mutants of SF-1 are shown. The *numbering* refers to the amino acid (aa) position. B, Flag-FOXL2 together with Myc-tagged WT or mutant SF-1 proteins were ectopically expressed in 293T cells, and their binding capacity was assessed by immunoprecipitation (IP) with α-Myc and α-FOXL2 antibodies. To assess expression of the respective proteins, Western blot (immunoblot, IB) analyses were conducted. Equal amounts of total protein were loaded in each lane, which was confirmed by the level of GAPDH expression.

abolished SF-1-induced *CYP17* gene activation (Fig. 3A). Next, we tested whether a FOXL2 mutant (1-53; Fig. 4A) found in a BPES type I patient with POF had lost its ability to inhibit the transcriptional activity of SF-1 and found that the mutant FOXL2 failed to repress *CYP17* transcription by SF-1 (Fig. 3A). Although LRH-1, the homolog of SF-1, also transactivated *CYP17*, FOXL2 did not block its activation activity (Fig. 3B), consistent with the lack of interaction observed between FOXL2 and LRH-1 (Fig. 1C). To determine whether FOXL2 also affects other target genes of SF-1, including *StAR*, *CYP11A1*, and *HSD3ß1*, SF-1, FOXL2, or both proteins were overexpressed in KGN cells, and real-time PCR analyses were conducted. The mRNA expression levels of *StAR*, *CYP11A1*, and *HSD3ß1* were significantly increased by SF-1, but the up-regulated expression of those transcripts were not significantly altered even after coexpression of FOXL2 (see Supplemental Fig. 1, published on The Endocrine Society's Journals Online web site at http://endo.endojournals.org).

Next, FOXL2 was depleted in KGN cells using a small interfering RNA (siRNA) specific for FOXL2 mRNA, and efficient knock-down of FOXL2 proteins was confirmed by immunoblot analysis (Fig. 3C). The transactivity of SF-1 on *CYP17* promoter activity increased by approximately 5-fold in the FOXL2-silenced cells compared with that in control cells receiving scrambled siRNA (Fig. 3D), demonstrating the repressive role of the endogenous FOXL2 protein on SF-1 activity.

To elaborate the functional relationship between WT FOXL2 and mutated forms of FOXL2, including those found in POF patients, on the repression of SF-1 activity, additional FOXL2 mutants lacking various functional domains were generated (Fig. 4A). We compared the ability of FOXL2 WT and mutants to repress SF-1-induced transactivity toward *CYP17* in primary granulosa cells isolated from immature rats. As shown in Fig. 4B, SF-1 produced a prominent transactivation of the *CYP17* promoter, and the stimulatory effect was completely blocked by FOXL2 overexpression. However, the FOXL2 mutants, 1-52 and 219-376, which both lacked the FH domain, lost the ability to repress the transcriptional activity of SF-1 on *CYP17* (Fig. 4B). Other FOXL2 mutants, which retained the FH domain (1-218 and 1-274) and are found in BPES patients, were able to inhibit SF-1-induced *CYP17* activation, but the suppression was significantly compromised compared with that of WT FOXL2 (Fig. 4B). Like WT FOXL2, a FOXL2 mutant lacking the alanine-rich region (ΔAla) retained the inhibitory effect, but the FH domain-deleted FOXL2 (ΔFH) not only failed to repress, but also further augmented, the transcriptional activation of *CYP17* by SF-1, implying that this mutant may even exist as a dominant negative form in rat granulosa cells (Fig. 4B). The WT or mutant FOXL2s did not significantly influence *CYP17* reporter gene expression (Fig. 4B). Thus, these data

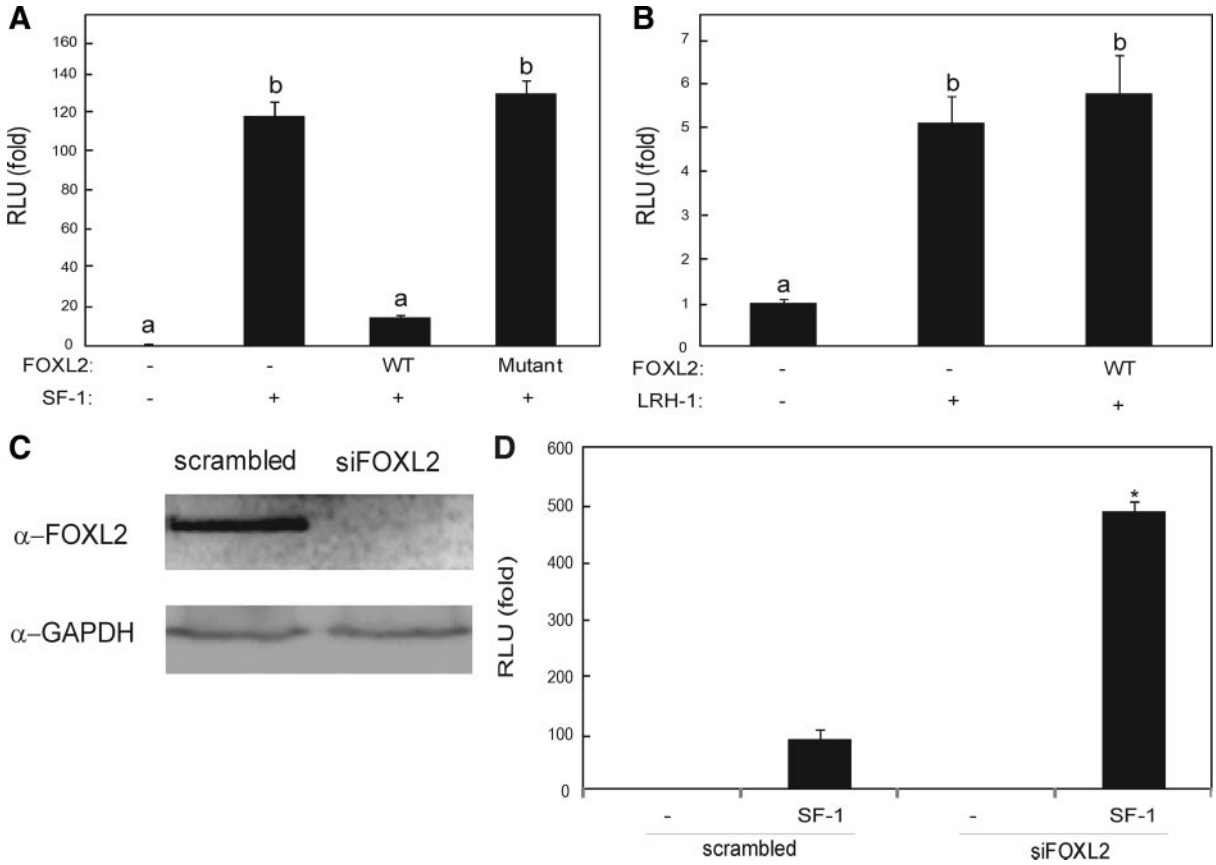

FIG. 3. Inhibitory role of FOXL2 on SF-1-induced *CYP17* promoter activation. A, Effects of FOXL2 and mutant FOXL2 (1–52) from a BPES type I patient on the transcriptional activity of SF-1 were investigated using a luciferase reporter system containing the *CYP17* promoter in KGN cells. Equal amounts of total DNA were used. As a control, cells were transfected with empty vector together with pGL3 *CYP17* promoter. Data are from three independent experiments conducted in triplicate and are presented as fold relative luciferase unit (RLU). Statistically significant values between groups are indicated with *different letters* ($P < 0.05$). B, Luciferase assays were performed as described in A by using LRH-1 instead of SF-1. Statistically significant values between groups are indicated with *different letters* ($P < 0.05$). C, Using a siRNA specific for FOXL2 mRNA, knock-down cells were produced, and reduced expression of endogenous FOXL2 in KGN cells was confirmed by immunoblot analysis. D, *CYP17*-luciferase reporter assays in FOXL2-depleted KGN cells were conducted as described in A. *Asterisks* indicate significant values compared with the control cells (−) transfected with an empty vector ($P < 0.05$).

demonstrate the importance of the FH domain for the inhibitory effect of FOXL2 on SF-1-induced *CYP17* transcriptional activation in that the mutated FOXL2s exhibit reduced activities.

Differential binding of FOXL2 and its mutants to SF-1

To investigate whether the defective inhibitory effects of the FOXL2 mutants on the transcriptional activation of *CYP17* by SF-1 could be due to altered binding capacity of the mutant forms of FOXL2 to SF-1, immunoprecipitation experiments were conducted in 293T cells. Two mutant forms of FOXL2 (1-218 and 1-274), which lacked sequences at the C terminus, retained the interaction with SF-1, but the N terminus-deleted (219-376) or FH-deleted (ΔFH) FOXL2 mutants lost their ability to bind to he SF-1 protein (Fig. 5A). The alanine region-deleted (ΔAla) FOXL2 mutant exhibited a reduced association with SF-1 (Fig. 5A). These binding assays suggest that the carboxyl end of FOXL2, including the alanine-rich region, is dispensable, but that the FH domain of FOXL2 is required for its association with SF-1. Because both mutants lacking the FH domain (218-376 and ΔFH) lost both the transcriptional repressive activity (Fig. 4B) and the capacity to interact with SF-1 (Fig. 5A), the FH domain of FOXL2 seems to be crucial in this context.

Subcellular localization of FOXL2 and its mutants

Because a previous study reported that mutations of FOXL2 lead to subcellular mislocalization and impaired transactivation (11), we investigated whether FOXL2 mutants failed to repress the transactivity of SF-1 by affecting the subcellular localization of SF-1. To determine the subcellular localization of FOXL2 mutants and SF-1, the nuclear and cytosolic fractions of 293T cell lysates were separated after overexpres-

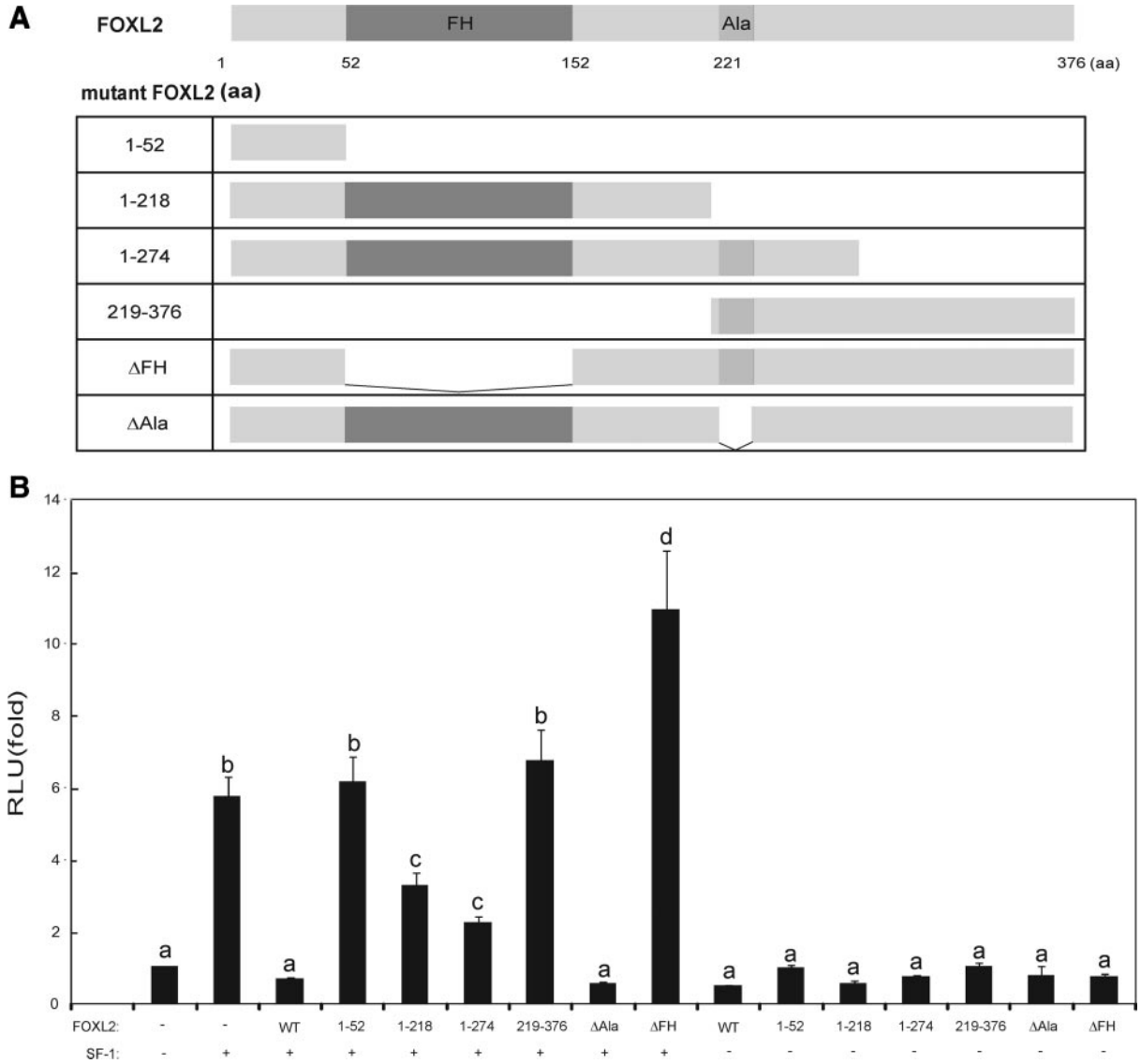

FIG. 4. Reduced activities of mutant FOXL2 with respect to the repression of SF-1-induced *CYP17* transcription. A, Mutant FOXL2 from BPES type I patients (1-52, 1-218, and 1-274) and artificial FOXL2 mutants are shown. The FH DBD and Ala repeat regions are indicated. B, The activities of mutant FOXL2s on SF-1-mediated *CYP17* transactivation in primary granulosa cells isolated from immature rats were assessed by luciferase reporter assays as in Fig. 3A. Statistically significant values between groups are indicated with *different letters* ($P < 0.05$).

sion of different forms of FOXL2 with or without SF-1. Efficient fractionation was determined by immunoblotting of histone H2B and ß-actin (Fig. 5B). Cellular localization of SF-1 and FOXL2 was also determined by fluorescence confocal microscopy (Fig. 5, C and D). The SF-1 protein was expressed in the nucleus, and its nuclear localization was not altered by FOXL2 overexpression (Fig. 5, B and D). WT and mutant FOXL2s were present in both the nuclear and cytosolic fractions, and their localization was not affected by SF-1 overexpression (Fig. 5, B–D). WT and mutant FOXL2s (1-218, 1-274, and ΔAla), which retained the FH domain, were largely present in the nuclear fraction (Fig. 5, B and C). In contrast, FOXL2 mutants (219-376 and ΔFH), which were devoid of the FH region, were mainly detected in the cytosolic fraction (Fig. 5, B and C).

Inhibition on SF-1-binding to the CYP17 promoter by FOXL2

To examine the possibility that the observed inhibition of FOXL2 on SF-1-induced CYP17 transcription observed (Fig. 3) could be due to interference of FOXL2 on the binding of SF-1 to CYP17, EMSA was performed using His-tagged purified recombinant FOXL2 and SF-1 proteins. The probe used contained known SF-1-binding sequences (Fig. 6A) at −211 to −204 (12). The SF-1 protein bound to the *CYP17* DNA probe, and no complex was found in the presence of an excess amount of cold competitor, whereas FOXL2 did not associate with the *CYP17* probe (Fig. 6B). Moreover, a dose-dependent loss of the SF-1-*CYP17* DNA complex by addition of increasing amounts of FOXL2 protein was observed, whereas incubation with an unrelated protein, BSA, did not dis-

rupt the association of SF-1 with *CYP17* DNA (Fig. 6B). Addition of anti-SF-1 antibodies weakened the formation of the SF-1-DNA complex, and supershift of SF-1-DNA complex was observed when antibodies to His-tag were added to the reaction (Supplemental Fig. 2).

Because *CYP19* (*aromatase*) transcription is known to be activated by SF-1 (13), as well as goat and fish Foxl2 (5, 14), we also examined how FOXL2 affects the binding of SF-1 to the *CYP19* promoter. In the presence of the FOXL2 protein, the formation of the SF-1 and *CYP19* probe complex was augmented (Supplemental Fig. 3A), and the enhanced complex formation between SF-1 and *CYP19* was observed by addition of FOXL2 protein in a dose-dependent manner (Supplemental Fig. 3B). In accordance, transactivation of SF-1-induced *CYP19* was significantly enhanced by coexpression of FOXL2, based on luciferase reporter assays (Supplemental Fig. 3C), demonstrating the distinct activities of FOXL2 toward different sets of target promoters. Furthermore, competition assays demonstrated that SF-1 has a higher affinity for *CYP19* over *CYP17* promoter (Supplemental Fig. 4).

Next, we investigated whether differential interference of the association between SF-1 and the *CYP17* promoter by WT and mutant FOXL2 could explain the defective inhibitory effects of FOXL2 mutants on SF-1-induced *CYP17* transcriptional activation. After cross-linking proteins and DNA, chromatin was isolated from KGN cells overexpressing SF-1 with or without FOXL2. The SF-1 protein was immunoprecipitated with anti-SF-1 antibodies, and PCR analysis was performed on the immunoprecipitated DNA using *CYP17* primer sets that encompassed the putative SF-1 binding sequences (Fig. 6A). Quantitative PCR from the immunoprecipitated chromatin revealed enrichment of the *CYP17* promoter fragments with SF-1 (Fig. 6C). In contrast, coexpression of FOXL2 abolished the enrichment of *CYP17* DNA fragments with SF-1 (Fig. 6C). Next, we assessed whether the inhibitory effects differ for the mutant forms of FOXL2 using a ChIP assay. In contrast to the WT, the mutant FOXL2 proteins (1-52, 219-376, and ΔFH), which lacked the transrepression activity toward SF-1-induced *CYP17* promoter activation as shown in Fig. 4B, was unable to inhibit the association of *CYP17* DNA and SF-1 (Fig. 6C). On the other hand, ΔAla FOXL2 efficiently blocked the SF-1-*CYP17* association in a similar manner to WT FOXL2 (Fig. 6C), supporting its intact transrepression activity to CYP17 mediated by SF-1 (Fig. 4B). The FOXL2 mutants showed partially compromised inhibition on SF-1-mediated *CYP17* transactivation (Fig. 6C). Thus, these results suggest that the difference in the inhibition of the association of SF-1 with *CYP17* may account for the differential *CYP17* transcriptional repression elicited by WT and mutant FOXL2s.

Discussion

Although mutant FOXL2 was discovered in women with POF in 2001 (1), only limited information regarding its target genes and signal transduction pathway is available so far. Here, we report that the human FOXL2 protein physically interacts with SF-1 and regulates the transcriptional activity of SF-1 on the expression of a steroidogenic enzyme, CYP17; meanwhile, the mutated FOXL2 found in patients shows impaired inhibitory activities on SF-1-induced transactivation of *CYP17* in ovarian cells.

SF-1, a member of the nuclear receptor superfamily, regulates various enzymes in steroid synthesis pathways of steroidogenic organs. The steroidogenic enzyme CYP17, also known as CYP17A1, P450c17, 17α-hydoxylase, or 17,20-lyase, converts pregnenolone and progesterone to 17-hydroxypregnenolone or 17-hydroxyprogesterone and further to dehydroepiandrosterone or androstenedione. Although studies have demonstrated the transactivity of SF-1 on *CYP17* expression in adrenal and testicular cells (15), it was unknown whether SF-1 also functioned accordingly in the ovary. In the present study, we demonstrated the transcriptional activation of *CYP17* by SF-1 in both human and rat granulosa cells (Figs. 3A and 4B).

Mice with granulosa cell-specific conditional knockout of SF-1 are sterile, have fewer follicles, lack corpora lutea, and have hemorrhagic cysts. These characteristics indicate the essential role of SF-1 in the ovary, which is possibly in estrogen production (16). Granulosa cells of small and preovulatory rodent ovarian follicles express SF-1, and this expression is modulated by gonadotropins (7). Therefore, SF-1 is likely to be a crucial factor for regulating the expression of enzymes involved in ovarian steroidogenesis. Consequently, any conditions that affect the transcriptional activities of SF-1 could disturb steroid hormone synthesis. In the present study, we found that forced expression of FOXL2 led to the complete inhibition of SF-1-induced *CYP17* up-regulation and that the transactivity of SF-1 was further enhanced in KGN cells lacking FOXL2 (Fig. 3, A and D). Strikingly, the mutant forms of FOXL2 found in POF patients exhibited either significantly compromised or abolished inhibitory effects on SF-1-mediated *CYP 17* transcription (Figs. 3A and 4B and Table 1). Thus, FOXL2 may restrain SF-1 activity to tightly control the production of sex hormones in the ovary, whereas in women expressing the truncated FOXL2 protein, normal production of sex steroid hormones may be disturbed. We previously reported that FOXL2 inhibits the transcription of *StAR*, an enzyme

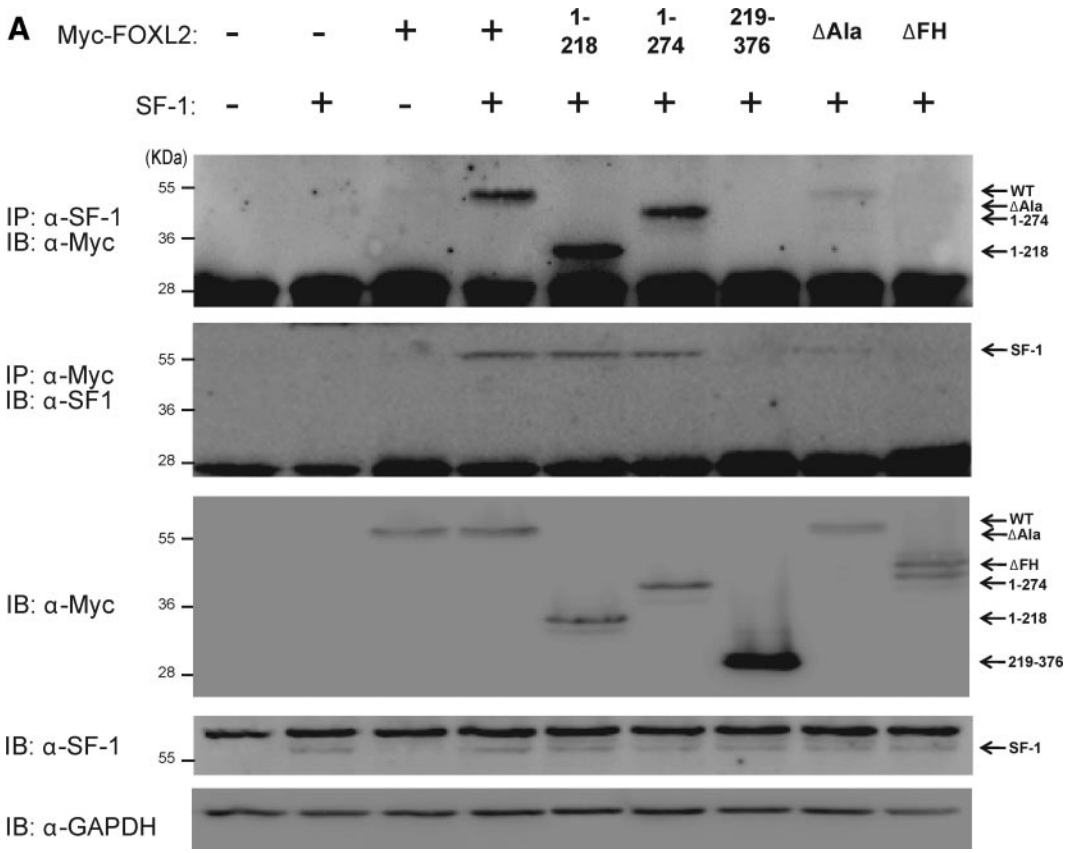

FIG. 5. Determination of SF-1 binding by mutant FOXL2s and their subcellular localization. A, Truncated FOXL2 mutants described in Fig. 4A were coexpressed with or without SF-1 in 293T cells. Immunoprecipitation (IP) experiments were conducted using α-SF-1 or α-Myc antibodies. Equal amounts of total protein from the cell lysates were used in each lane. Lysates were prepared 24 h after transfection, separated into nuclear and cytosolic fractions, and immunoblotted (IB) with the respective antibodies. B, The 293T cells overexpressed WT or mutant FOXL2 with or without SF-1. Lysates were prepared 24 h after transfection, separated into heavy membrane and cytosolic fractions, and immunoblotted with the respective antibodies. C, Myc-tagged WT and mutated FOXL2 were overexpressed in 293T cells, and fluorescence confocal microscopy images are shown. Myc-FOXL2s were visualized using Alexa Fluor 546 goat antimouse IgG. Visualization of nucleus was determined using 4′,6-diamidino-2-phenylindole (DAPI). D, Myc-FOXL2s were coexpressed with SF-1 in 293T cells, and the FOXL2s and Flag-tagged SF-1 proteins were visualized using Alexa Fluor 546 goat antimouse IgG or Alexa Fluor 488 goat antirabbit IgG, respectively.

required for the initial step of steroidogenesis, whereas its mutants fail to do so (2). Recently, the Nagahama group reported the association of tilapia Sf-1 with Foxl2, although they did not directly show binding of the two proteins *in vivo* (5). They found that tilapia fish Foxl2 stimulates tilapia *Cyp19a1*, an aromatase gene, and further enhances Sf-1-induced *Cyp19a1* transactivation in the mouse testicular cell line TM3. In addition, the transactivity of Sf-1 on medaka *P450c17s* was enhanced by medaka Foxl2 in HEK 293 cells (17). The varied effects observed may be partly due to the differences in species and/or cell types used.

To investigate the underlying mechanism by which WT and mutant FOXL2s display differential inhibitory effects on SF-1 activity, their protein-protein interactions were determined (Table 1). Comparative analyses of *in vivo* binding and promoter activity results (Figs. 4B and 5A) indicate, that although the association between FOXL2 and SF-1 seems to be necessary for FOXL2 or its mutants to inhibit SF-1-mediated CYP17 transactivation, a weaker interaction between them is possibly sufficient to repress SF-1 activity, especially considering the effects of the ΔAla mutant (Table 1). Moreover, the compromised transcriptional repression observed for mutant FOXL2 proteins is not likely a direct consequence of altered binding capacity between the mutants and SF-1, but other elements seem to be involved. Thus, next, we tested the possibility of discriminative actions by WT and mutated FOXL2s in the association of SF-1 with the *CYP17* promoter. According to the EMSA and ChIP data, FOXL2 drastically inhibited the enrichment of *CYP17* DNA on SF-1, whereas the mutant FOXL2 found in POF patients completely or partially failed to block the association of SF-1 with *CYP17* (Fig. 6, B and C, and Table 1). These observations corroborate with the finding of the observed differential inhibitory activities of WT and mutants FOXL2 on SF-1-induced transcriptional activation of CYP17 (Fig. 4B). At this point, it is unclear exactly how FOXL2 hinders the binding of SF-1 to the promoter of *CYP17*. However, based on our observation that the

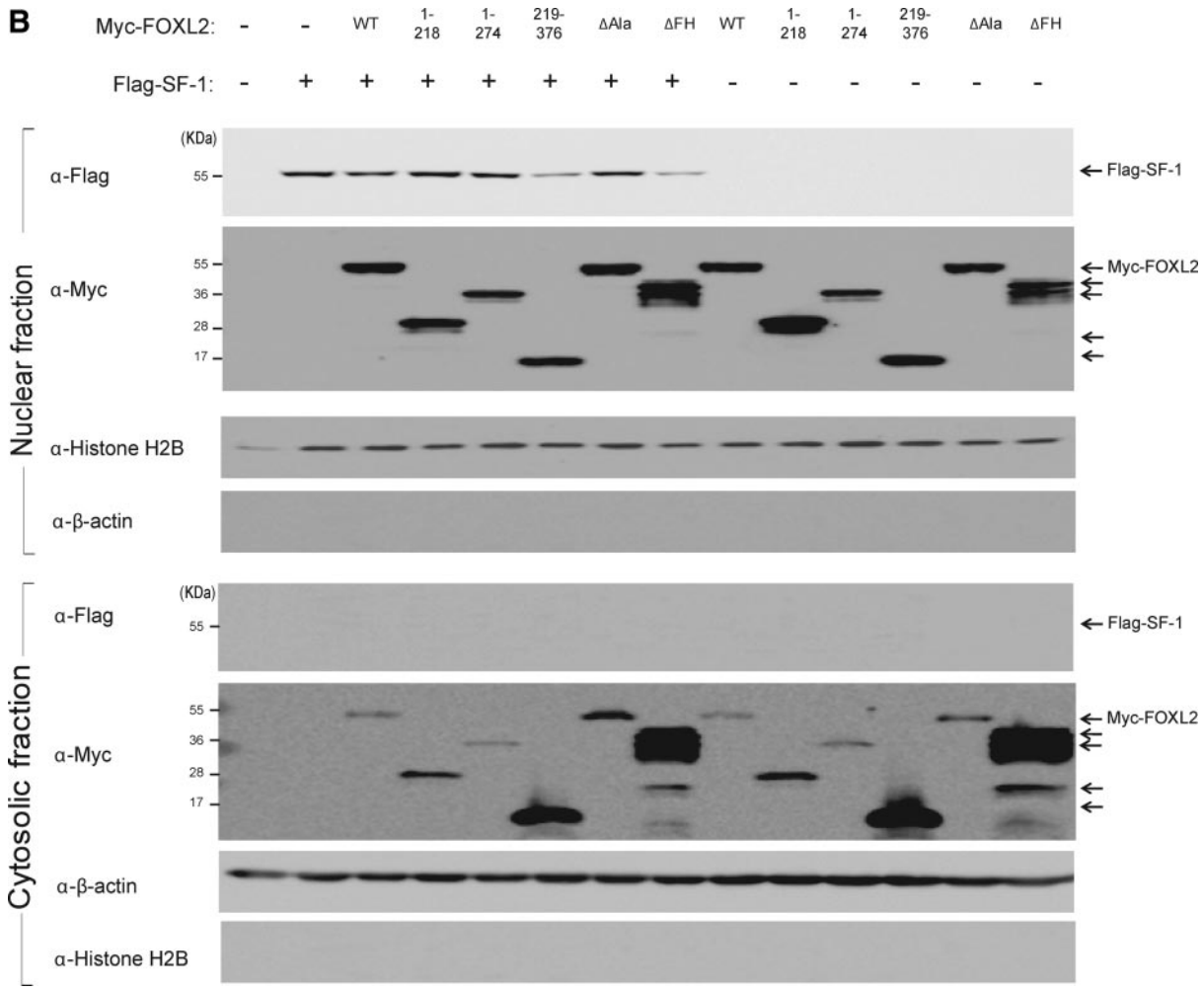

FIG. 5. *Continued.*

DNA binding domain of SF-1 is essential for its interaction with FOXL2 (Fig. 2B), the binding of FOXL2 to the DNA binding domain of SF-1 may subsequently affect the association of SF-1 with *CYP17* by masking the promoter-binding region. Concurrently, the engagement of FOXL2 with the SF-1 protein may also influence the association between SF-1 and other cofactors that might be necessary for the proper transcriptional activity of SF-1. Even though the present study attempted to decipher the repressive activity of FOXL2 on SF-1, the reciprocal action of SF-1 to regulate unknown target genes of FOXL2 is possible and should be evaluated in future studies.

Genotype-phenotype correlation for intragenic mutations of FOXL2 has been proposed. Mutations predicted to produce truncated proteins before the poly-Ala region would be associated with BPES type I, whereas poly-Ala expansion would result in BPES type II (18). The current luciferase reporter assays performed with different FOXL2 mutants support this prediction. Compared with the observed transcriptional repression by WT FOXL2 on SF-1-induced *CYP17* activation, the mutant lacking both the FH domain and the poly-Ala tract (1-52) completely failed to repress *CYP17* transcription (loss-of-function), whereas another FOXL2 mutant possessing both the FH domain and the Ala repeats retained its ability to inhibit *CYP17* transactivation, although the effect was diminished (Fig. 4B). Interestingly, the FH-deleted mutant FOXL2 (ΔFH) not only lost its inhibitory effect on SF-1-induced *CYP17* activation, but also further increased transactivation by SF-1, whereas the alanine-deleted FOXL2 mutant (ΔAla) retained its repressive activity (Fig. 4B). Based on these data, the FH domain, but not the poly-Ala region, of FOXL2 is important and likely essential and responsible for the transcriptional repression of SF-1 at *CYP17*.

POF is a complex disease, and the etiology of most cases of POF is idiopathic and very heterogeneous (19). The two fundamental mechanisms of POF include either a failure to attain the appropriate peak follicle number or an accelerated loss of the oocyte and follicle pool (20). Recently, different genetically modified mouse models of POF have been established, which is expected to aid in understanding ovarian failure in women (21). Despite the fact that all of the gene knockout mouse models exhibit

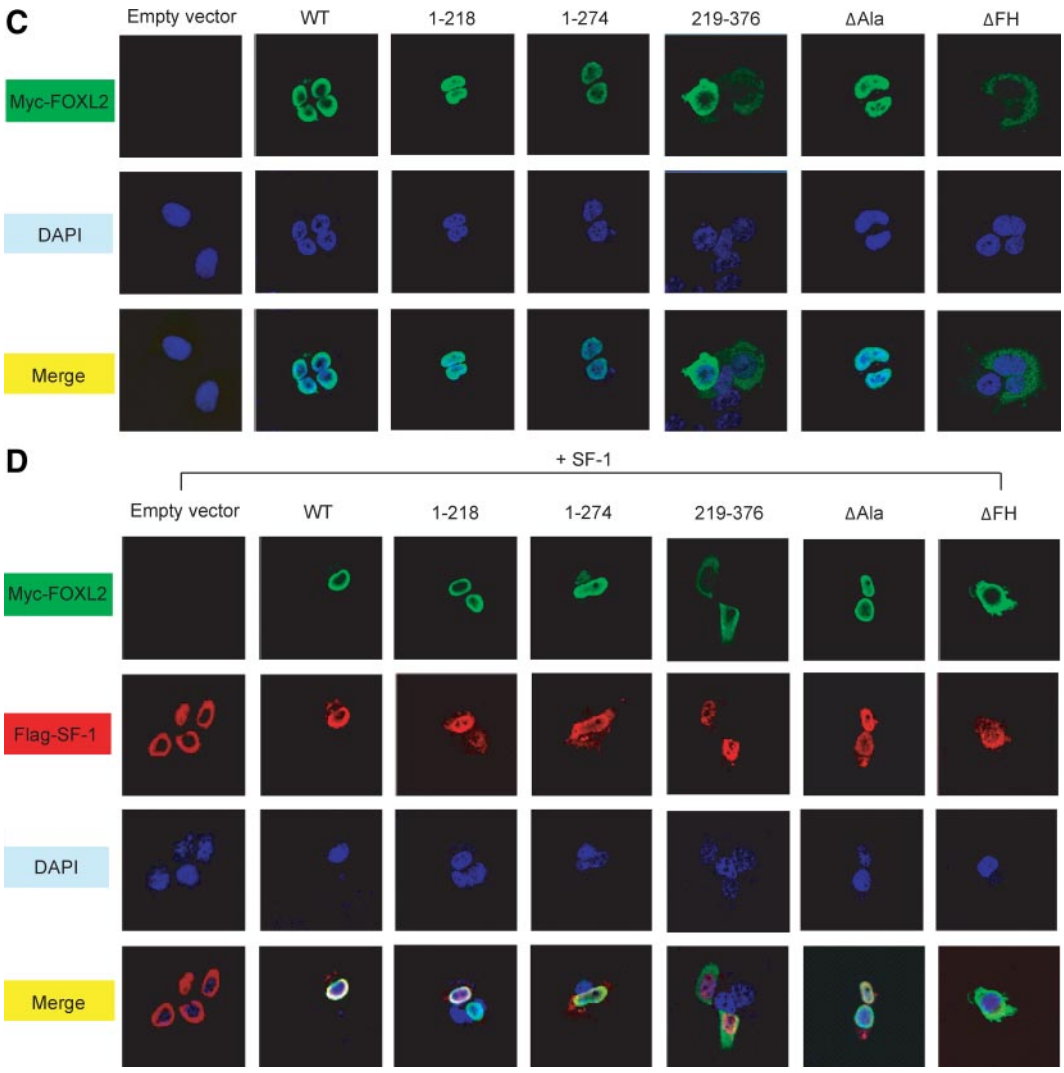

FIG. 5. *Continued.*

some degree of ovarian failure output, the spatial and temporal expression patterns of the genes, the detailed manifesting phenotypes in the ovaries, and the underlying mechanisms by which the deletion of genes affecting normal ovarian function are extremely heterogeneous (19, 21, 22). The distinct phenotype of FOXL2 null mice suggests a failure of granulosa cell differentiation, leading to premature follicle activation and consequent depletion (4), and SF-1 positively regulates the differentiation of rat granulosa cells (23). Temporal expressions of FOXL2 and CYP17 in the course of follicle development agree, because the level of FOXL2 is higher in primordial and primary follicles in which CYP17 is not detectable (4, 24).

In the current study, we identified SF-1 as an endogenous binding partner of FOXL2 in human ovarian cells. FOXL2 acts as a suppressor of SF-1, leading to the inhibition of the transcriptional activation of *CYP17* in granulosa cells, whereas mutated FOXL2 proteins found in women with BPES type I with POF lost the inhibitory activity against *CYP17* induction by SF-1. Therefore, this study presents previously unknown targets of FOXL2 and provides their regulatory network. Although we proved differential activities between WT and mutant FOXL2 toward SF-1, more evidence is required to determine whether this signaling network accounts for the ovarian pathogenesis of the truncated forms of FOXL2.

Materials and Methods

Chemicals and reagents

Unless otherwise indicated, reagents were purchased from Sigma (St. Louis, MO).

Plasmid constructions

The SF-1 encoding plasmid and the human *CYP17* promoter plasmid were generous gifts from K. Parker (University of Texas Southwestern Medical Center, Dallas, TX) and J. Richards (Baylor College of Medicine, Houston, TX), respectively. The plasmid encoding FOXL2 was cloned as described previously (9), and the HA-tagged LRH-1 expression vector was kindly provided by H. S. Choi (Chonnam National University, Gwangju, Korea). Flag-

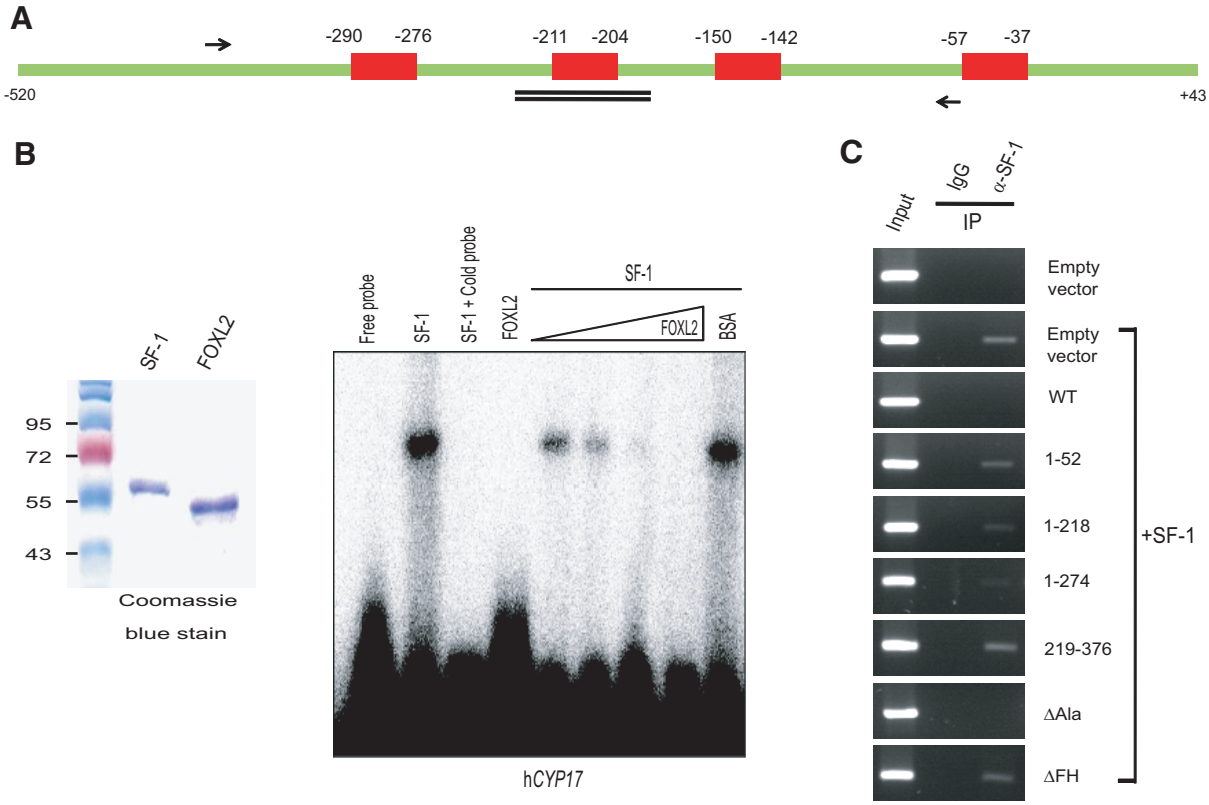

FIG. 6. Disturbance of SF-1 recruitment to *CYP17* by FOXL2. A, The *CYP17* promoter region with SF-1-binding elements (*red*) is shown. The region of *CYP17* probe sequences used in EMSA is indicated by *two parallel lines*, and the primer pair used for PCR amplification is indicated with *arrows*. B, Coomassie blue staining of the purified recombinant His-tagged SF-1 and FOXL2 proteins are shown (*left panel*). The recombinant SF-1 (1.0 μg) was incubated in the presence of increasing amounts of FOXL2 protein (0.1, 0.25, 0.5, and 1.0 μg) with radiolabeled double-stranded oligonucleotides corresponding to the *CYP17* promoter (*right panel*). Cold probe (×100) and BSA (1.0 μg) were also included to examine the specificity of the complex formation. C, KGN cells were transfected with plasmids encoding SF-1 together with WT or mutated FOXL2, and ChIP was performed using an α-SF-1 antibody. Using the precipitated chromatin fragment, PCR was conducted with a set of *CYP17*-specific primers that encompassed the SF-1-binding elements. The PCR products were electrophoresed in an agarose gel and visualized. As a negative control, normal IgG was used in the ChIP assays. A representative gel picture from three independent experiments is shown.

tagged FOXL2 was produced by PCR amplification using the following primers: pcFlag-hFOXL2-F (5′-AGTGGATCCATGGACTACAAAGACGACGACGACAAAGCCAGCTACCCCGAGCCC) and FOXL2-R (5′-CTACTCGAGTCAGAGATCGAGGCGCGA) and cloned into pcDNA3. pCMV Myc-tagged (CLONTECH, Mountain View, CA) FOXL2 was cloned after PCR amplification using the following primers: FOXL2-F (5′-CTAGAATTCAAATGATGGCCAGCTACCCC) and FOXL2-R (5′-CTACTCGAGTCAGAGATCGAGGCGCGAATG). Mutant forms of FOXL2 were cloned into pCMV Myc after PCR amplification using the respective primer sets: FOXL2 (1-52) with FOXL2-F and FOXL2 52-R (5′-CTACTCGAGTCACGCCGGGTCCGGCTTCTC); FOXL2 (1-218) with FOXL2-F and FOXL2 218-R (5′-CTACTCGAGTCAGCAGGAGGCATAGGGCAT); FOXL2 (1-274) mutant with FOXL2-F and FOXL2 274-R (5′-CTACTCGAGTCAGTACGAGTTCACTACGCC); and FOXL2 (218-376) mutant with FOXL2 218-F (5′-CTAGAATTCAAATGCAGATGGCGGCAGCCGC) and FOXL2-R. The ΔAla FOXL2 and the ΔFH FOXL2 constructs were produced by a recombinant PCR technique using the following primers: ΔAla FOXL2 with FOXL2-F, ΔAla FOXL2-R (5′-CCGCGCCAGGGCTACCGGGCTGGCAGGAGGCATAGG),

TABLE 1. Summary of properties of WT and mutant FOXL2s

FOXL2 WT and mutants	Binding to SF-1	Major cellular localization	Repression of SF-1-induced *CYP17* transactivity	Inhibition of SF-1-CYP17 complex formation
WT	+++	N	+++	+++
1-52	n.d.	n.d.	–	–
1-218	+++	N	++	++
1-274	+++	N	++	++
219-376	–	C	–	–
ΔAla	+	N	+++	+++
ΔFH	–	C	––	–

Plus sign, Positive action; *more than one plus sign*, stronger positive action; *minus sign*, negative action; *more than one minus sign*, stronger negative action; n.d., not determined due to small size; N, nuclear; C, cytosolic.

ΔAla FOXL2-F (5′-CCCGGTAGCCCTGGCGCGGCCGCTGTG), and FOXL2-R; and ΔFH FOXL2 with FOXL2-F, ΔFH FOXL2-R (5′-CGGCCGGAAGGGCCTCTTCTGCGCCGGGTCCGGCTT), ΔFH FOXL2-F (5′-AAGAGGCCCTTCCGGCCGCCGCCCGCG), and FOXL2-R. Flag-tagged pcDNA3 SF-1 was PCR amplified using the following primers: pcFlag-hFOXL2-F (5′-AGTGGATCCATGGACTACAAAGACGACGACGACAAAGACTATTCGTACGAGAG) and SF-1-R (5′-CTACTCGAGTCAAGTCTGCTTGGCTTG). pCMV HA (CLONTECH) SF-1 was cloned after PCR amplification using the following primers: CMV SF-1-F (5′- CTAGAATTCAAATGGACTATTCGTACGACGAG) and CMV SF-1-R (5′-CTACTCGAGTCAAGTCTGCTTGGCTTG). Truncated SF-1 plasmids were PCR amplified using respective sets of the following primers: SF1 (1-240) with CMV SF-1-F and CMV SF-1 240-R (5′-CTA CTCGAGTCACCGCAACACCAGGCTGTG); SF-1 (1-355) with CMV SF-1-F and CMV SF-1 355-R (5′-CTACTCGAGTCAGTACGAGTTCACTACGCC); SF-1 (220-461) with CMV SF-1 220-F (5′-CTAGAATTCAAATGCCCAACGTGCCTGAGCTC) and CMV SF-1-R; and SF-1 (90-461) with CMV SF-1 90-F (5′-CTAGAATTCAAATGGGTGGCCGGAACAAGTTT), and CMV SF-1-R. PCR products were digested with *Eco*RI and *Xho*I (Roche, Pleasanton, CA) and ligated to pCMV Myc or HA vectors. For bacterial expression of SF-1 and FOXL2 proteins, pCMV Myc-SF-1 and pCMV Myc-FOXL2 were digested with *Eco*RI, blunt-ended using Klenow DNA polymerase (Roche), digested with *Not*I or *Xho*I, respectively, and ligated into pET28a (Novagen, San Diego, CA).

Production of FOXL2 antibodies

Polyclonal FOXL2 antibodies were raised and purified against a synthetic human FOXL2 peptide (GRTVKEPEGPPPSPGKC) (AbFrontier, Seoul, Korea), and the antibody titer was determined by the peptide-specific enzyme-linked immunosorbent assay.

Animals and rat granulosa cell isolation

Immature female Sprague Dawley rats (15–18 d old) were purchased from Samtako (Osan, Korea), housed at CHA University animal facilities, and maintained in accordance with guidelines provided and protocols approved by the Institutional Animal Care and Use Committee of CHA University; 21-d-old rats were injected sc with 20 mg of diethylstilbesterol daily for 3 d. Ovaries were isolated from diethylstilbesterol-treated 24-d-old rats, placed in a Petri dish containing Leibovitz medium (GIBCO, Gaithersburg, MD) and 0.1% BSA (Bovogen, Essendon, Australia), transferred to a new dish, and punctured with a 1-ml syringe needle (Kovax, Ansan, Korea). Granulosa cells were collected by centrifugation (160 × g) for 3 min and washed with McCoy medium (Welgene, Seoul, Korea).

Mammalian cell culture

The 293T and human granulosa KGN cells were cultured in DMEM (Welgene) and DMEM/F12 medium (Welgene), respectively. KGN cells were provided by Yoshihiro Nishi and Toshihiko Yanase (Kyushu University, Fukuoka, Japan). Primary granulosa cells were incubated in McCoy medium. All media contained 10% fetal bovine serum (FBS) (PAA, Etobicoke, Canada) and 1% penicillin-streptomycin (Welgene).

Immunoprecipitation and Western blot analysis

The 293T cells (3.0×10^6) were transfected with a total of 6 μg of the respective plasmid DNA using Welfect-EX PLUS (Welgene) in 100-mm dishes. Cell lysates were prepared with Nonidet P-40 (NP-40) lysis buffer (50 mM Tris-HCl, at pH 8.0; 0.15 M NaCl; and 1% NP-40) containing 10% protease inhibitor cocktail. The lysates were centrifuged, and the supernatants were precleared with normal IgG (Santa Cruz Biotechnology, Inc., Santa Cruz, CA) and protein G-agarose (Upstate, Charlottesville, VA) for 2 h at 4 C. Precleared lysates were incubated with primary antibodies for 12 h followed by incubation with protein G-agarose for an additional 1 h at 4 C. Immune complexes were centrifuged and washed three times with NP-40 lysis buffer. For quantitative protein analysis, a standard curve was established with a standard BSA solution (Pierce, Rockford, IL), and equal amounts of total protein were subjected to SDS-PAGE. After transferring the proteins to nitrocellulose membranes, the membranes were blocked with 5% nonfat milk. HA-tagged WT SF-1 and its mutant forms were detected with an anti-HA monoclonal antibody, Myc-tagged WT FOXL2 and its mutant proteins were detected with an anti-Myc monoclonal antibody, and Flag-tagged FOXL2 was detected with rabbit anti-Flag antibodies. For the detection of endogenous FOXL2 and SF-1 proteins in KGN cells (1.0×10^7), anti-FOXL2 or anti-SF-1 polyclonal antibodies (Santa Cruz Biotechnology, Inc.) were used, respectively. As loading controls, glyceraldehyde-3-phosphate dehydrogenase (GAPDH) and ß-actin were analyzed by Western blotting with anti-GAPDH (AbFrontier) and anti-ß-actin (Santa Cruz Biotechnology, Inc.), respectively. Membranes were stripped by incubation in stripping buffer [100 mM mercaptoethanol; 2% sodium dodecyl sulfate (SDS); and 62.5 mM Tris-HCl, at pH 6.8] at 50 C for 30 min and were washed with PBS (137 mM NaCl; 2.7 mM KCl; 10 mM Na_2HPO_4; and 2 mM KH_2PO_4, at pH 7.4) containing 0.01% Tween 20 (PBS-T). Membranes were incubated with horseradish peroxidase-conjugated antimouse IgG secondary antibodies (Santa Cruz Biotechnology, Inc.) at room temperature for 1 h, before visualization with enhanced chemiluminescence (AbFrontier). Proteins were detected using the LAS Image program (Fuji, Tokyo, Japan).

Quantification of mRNA

KGN cells (2.4×10^6) were transfected with a total of 6 μg of the plasmids encoding FOXL2 and/or SF-1 and pcDNA3 empty vector using a MicroPorator MP-100. Total RNA was extracted from KGN cells using an Intron Total RNA Extraction kit (Intron, Seungnam, Korea). The concentration and quality of RNA were determined with a ND-1000 spectrophotometer (NanoDrop, Waltham, MA). Reverse-transcription to cDNA was conducted using the SuperScriptIII First-Strand Synthesis System kit (Invitrogen, Carlsbad, CA) and following the manufacturer's instructions. All cDNAs used in real-time PCR were normalized with GAPDH. Quantitative real-time PCR was performed using a SYBR Green I kit (QIAGEN, Hilden, Germany), using the housekeeping gene GAPDH as a control. Real-time PCR was performed in a Rotor-Gene 3000 (Corbett Research, Sydney, Australia), and gene expression was quantified by the ΔΔCt method. Nucleotide sequences of the primers were as follows: GAPDH-F (5′-AGCCAAAAGGGTCATCATCTCT), GAPDH-R (5′-AGGGGCCATCCACAGTCTT), HSD3ß1-F (5′-CGGCCTCCGCCTTGATTCCA), HSD3ß1-R (5′-ATGTGGCGGTTGAAGGGCGG), StAR-F (5′-GGGGGAGGAGGCCATGCAGA), StAR-R (5′-GCCGGAACACCTTGCCCACA), CYP11A1-F (5′-GGCAGGAGGGGTG-

GACACGA), and CYP11A1-R (5′-GGCCATGTCTCCCT-GGGCCT).

Luciferase assay

KGN cells (4×10^5) were transfected with 170 ng of the pCMV β-galactosidase plasmid (CLONTECH), 300 ng of the *CYP17*-responsive luciferase reporter, and plasmids encoding FOXL2 and/or SF-1 using a MicroPorator MP-100 (Digital Bio Technology, Seoul, Korea). Cells were then incubated in 12-well plates containing fresh DMEM/F12 medium for 24 h. For the reporter assay using immature rat granulosa cells, cells (3×10^5) were transfected with 50 ng of pCMV β-galactosidase, 250 ng of the *CYP17*-responsive luciferase reporter, 125 ng of pcDNA3 SF-1, and 125 ng of FOXL2 using Metafectene (Biontex, Martinsried, Germany) following the manufacturer's instructions. Cells were then incubated in McCoy medium with 1% FBS and 1% penicillin-streptomycin for 24 h. Cells were washed with PBS and lysed with 100 μl/well of Reporter Lysis buffer (Promega, Madison, WI). Luciferase activity was measured using the Luciferase Assay System kit (Promega) and normalized to β-galactosidase activity. The absorbance was measured with the PerkinElmer 1420 Multilabel Counter (PerkinElmer, Waltham, MA).

Subcellular fractionation

The 293T cells (1×10^7) were transfected with 6 μg of plasmids encoding FOXL2 and/or SF-1 using Welfect-EX PLUS in 100-mm dishes for 24 h. After the cells were washed twice with cold PBS, the cells were lysed with cytosolic extraction buffer A (10 mM HEPES, at pH 7.9; 10 mM KCl; and 0.1 mM EDTA) containing 1 mM dithiothreitol (DTT), 10% Igepal CA-630, and 10% protease inhibitor cocktail and incubated for 5 min at room temperature. After centrifugation, the supernatants were separated from the pellets, which were solubilized in nuclear lysis buffer B (20 mM HEPES, at pH 7.9; 0.4 M NaCl; 1 mM EDTA; and 10% glycerol) containing 1 mM DTT and protease inhibitor cocktail and centrifuged at 10,000 × *g* for 10 min at 4 C. Antibodies against β-actin (Santa Cruz Biotechnology, Inc.) and histone H2B (Santa Cruz Biotechnology, Inc.) were incubated with the cytosolic or nuclear fractions, respectively.

Immunofluorescence analysis

The 293T cells (2×10^4) were seeded onto round cover slips in 24-well plates. After 24 h of incubation, 200 ng each of pcDNA3 Flag-SF-1 and pCMV Myc-FOXL2 WT and mutants were transfected into the cells. At 18 h after transfection, cells were fixed with 4% paraformaldehyde for 15 min at room temperature. The fixed cells were permeabilized with 0.2% Triton X-100 in PBS and then incubated with 2% FBS in PBS for 1 h. Fixed cells were incubated for 1 h with primary antibodies in PBS-T. Anti-Flag (1:100) and anti-Myc (1:100) antibodies were used to detect the localization of SF-1 and FOXL2, respectively. After washing three times with PBS-T, the cells were counterstained with Alexa Fluor 546 goat antimouse IgG (1:1000) (Invitrogen), Alexa Fluor 488 goat anti-rabbit IgG (1:1000) (Invitrogen), and Hoechst 33342 (1:300) (Invitrogen) for 1 h. After additional washing with PBS-T, the stained round glass cover slips were mounted on slides using mounting solution. Fluorescence was detected using a Zeiss LSM 510 META confocal microscope (Carl Zeiss, Göttingen, Deutschland).

Recombinant protein purification

His-tagged SF-1 and FOXL2 proteins were produced by induction of T7 RNA polymerase in *Escherichia coli* strain BL21(DE3) containing pET28a-SF1 or pET28a-FOXL2, respectively. Cells were cultured in Luria-Bertani medium containing 100 μg/ml kanamycin and grown at 30 C until $OD_{600} = 0.3$ when 200 μM of isopropyl β-D-thiogalactoside was added. The cells were harvested after an additional hour of culture, then pelleted and resuspended in lysis buffer containing 5 mM imidazole, and lysed with a French press. The lysates were cleared by centrifugation (12,000 × g) for 20 min at 4 C to remove cell debris. SF-1 and FOXL2 proteins were purified by affinity chromatography with Ni-NTA agarose (QIAGEN, Valencia, CA) on Econo-Pac columns (Bio-Rad, Hercules, CA) and then eluted with an imidazole gradient (5–400 mM). The buffer in the purified protein samples were replaced with storage buffer [20 mM HEPES, at pH 7.9; 400 mM NaCl; 1 mM EDTA; 1.5 mM $MgCl_2$; and 10% (vol/vol) glycerol] using Centricon YM-50 filter devices (Millipore, Bedford, MA).

EMSA

Double-stranded oligonucleotides of hCYP17 (−211/−204) and hCYP19 (−136/−124), 5′-GGTGATCAACTGACCTC-CCTTACCTAG-3′ and 5′-TGAGACTCTACCAAGGTCA-GAAATGCT-3′, respectively, were radiolabeled with [γ-^{32}P]ATP (3000 Ci/mmol) using T_4 polynucleotide kinase (10 U/μl) (Takaka Bio, Otsu, Japan) at 37 C for 30 min. Approximately 20 fmol of ^{32}P-labeled probes and 1 μg of the purified proteins were incubated for 1 h at 30 C in a reaction mixture containing 250 mM NaCl; 50 mM Tris-Cl, pH 7.5; 5 mM $MgCl_2$; 1 mM DTT; 50 μg/ml BSA; and 10% (vol/vol) glycerol. For the supershift assay, anti-SF-1 and anti-His (Santa Cruz Biotechnology, Inc.) antibodies were added, and the reactions were incubated for an additional hour on ice. The reaction products were analyzed by electrophoresis on a 6% nondenaturing polyacrylamide gel.

ChIP analysis

KGN cells (2×10^7) were electroporated with plasmids using a MicroPorator MP-100, incubated in 100-mm dishes for 24 h, and cross-linked with 1% formaldehyde for 10 min at room temperature. The reaction was terminated by the addition of glycine (final concentration, 0.125 M) for 5 min at room temperature. Cells were scraped in cold PBS containing protease inhibitor cocktail, collected by centrifugation (5000 × g for 10 min at 4 C), and incubated for 10 min on ice in SDS lysis buffer (50 mM Tris-HCl, at pH 8.1; 10 mM EDTA; and 1% SDS) containing protease inhibitor cocktail. The lysates were then sonicated on ice to a mean length of 500-1000 bp and centrifuged at 12,000 × g at 4 C for 10 min. The chromatin solution was diluted in buffer containing 0.01% SDS, 1.1% Triton X-100, 1.2 mM EDTA, 16.7 mM Tris-HCl (pH 8.1), and 167 mM NaCl and then precleared with a protein G-agarose and normal rabbit IgG slurry (Santa Cruz Biotechnology, Inc.) for 1 h at 4 C with rotation. Input samples were obtained followed by immunoprecipitation with anti-SF-1, overnight at 4 C with rotation. Immune complexes were collected using protein G-agarose slurry for 1 h at 4 C with rotation and sequentially washed for 2 min each in low salt wash buffer [0.1% SDS, 1% Triton X-100, 2 mM EDTA, 20 mM Tris-HCl (pH 8.1), and 150 mM NaCl], high salt wash buffer [0.1% SDS, 1% Triton X-100, 2 mM EDTA, 20 mM Tris (pH 8.1), and 500 mM NaCl], LiCl wash buffer [0.25 M LiCl, 1% Igepal CA-630, 1% deoxycholic acid, 1 mM EDTA, and 10 mM Tris-HCl (pH 8.1)], and two washes with Tris/EDTA buffer [10 mM Tris-HCl (pH 8.0) and 1 mM EDTA (pH 8.0)]. Precipitates were then extracted two times with elution buffer (1% SDS and 0.1 M $NaCO_3$). Eluates were pooled, and cross-linking was reversed by incubation at 65 C overnight. Unbound proteins were

digested with proteinase K (Promega) for 2 h at 45 C, and chromatin was purified using the DNA Clean-up kit (GeneAll Biotechnology, Seoul, Korea). DNA was amplified using a primer set flanking the SF-1 binding motifs in the *CYP17* promoter: sense (5′-ATGGAGCAAGACTCTGAA-3′) and antisense (5′-TTCCACAAGGCAAGAGAT-3′). Products were separated on agarose gels containing ethidium bromide.

Statistical analysis

Multiple comparison analyses of values were performed with the Student-Newman-Keul's test (SAS, Cary, NC), and significance of values was analyzed by compared with the controls was determined with the Student's *t* test.

Acknowledgments

Address all correspondence and requests for reprints to: Jeehyeon Bae, Department of Biomedical Science, College of Life Science, CHA University, Seongnam 463-836, Korea. E-mail: jeehyeon@cha.ac.kr.

This work was supported by the Basic Science Research Program (2009-0066320) and the Priority Research Centers Program (2009-414-E00006) through the National Research Foundation of Korea funded by the Ministry of Education, Science, and Technology; by the Korea Healthcare Technology R&D Project funded by the Ministry of Health, Welfare, and Family Affairs Grant A084923; and by the Seoul R&BD program (10543 and 10550).

Disclosure Summary: The authors have nothing to disclose.

References

1. **Crisponi L, Deiana M, Loi A, Chiappe F, Uda M, Amati P, Bisceglia L, Zelante L, Nagaraja R, Porcu S, Ristaldi MS, Marzella R, Rocchi M, Nicolino M, Lienhardt-Roussie A, Nivelon A, Verloes A, Schlessinger D, Gasparini P, Bonneau D, Cao A, Pilia G** 2001 The putative forkhead transcription factor FOXL2 is mutated in blepharophimosis/ptosis/epicanthus inversus syndrome. Nat Genet 27:159–166
2. **Pisarska MD, Bae J, Klein C, Hsueh AJ** 2004 Forkhead l2 is expressed in the ovary and represses the promoter activity of the steroidogenic acute regulatory gene. Endocrinology 145:3424–3433
3. **Uda M, Ottolenghi C, Crisponi L, Garcia JE, Deiana M, Kimber W, Forabosco A, Cao A, Schlessinger D, Pilia G** 2004 Foxl2 disruption causes mouse ovarian failure by pervasive blockage of follicle development. Hum Mol Genet 13:1171–1181
4. **Schmidt D, Ovitt CE, Anlag K, Fehsenfeld S, Gredsted L, Treier AC, Treier M** 2004 The murine winged-helix transcription factor Foxl2 is required for granulosa cell differentiation and ovary maintenance. Development 131:933–942
5. **Wang DS, Kobayashi T, Zhou LY, Paul-Prasanth B, Ijiri S, Sakai F, Okubo K, Morohashi K, Nagahama Y** 2007 Foxl2 up-regulates aromatase gene transcription in a female-specific manner by binding to the promoter as well as interacting with ad4 binding protein/steroidogenic factor 1. Mol Endocrinol 21:712–725
6. **Luo X, Ikeda Y, Parker KL** 1994 A cell-specific nuclear receptor is essential for adrenal and gonadal development and sexual differentiation. Cell 77:481–490
7. **Falender AE, Lanz R, Malenfant D, Belanger L, Richards JS** 2003 Differential expression of steroidogenic factor-1 and FTF/LRH-1 in the rodent ovary. Endocrinology 144:3598–3610
8. **Parker KL, Rice DA, Lala DS, Ikeda Y, Luo X, Wong M, Bakke M, Zhao L, Frigeri C, Hanley NA, Stallings N, Schimmer BP** 2002 Steroidogenic factor 1: an essential mediator of endocrine development. Recent Prog Horm Res 57:19–36
9. **Lee K, Pisarska MD, Ko JJ, Kang Y, Yoon S, Ryou SM, Cha KY, Bae J** 2005 Transcriptional factor FOXL2 interacts with DP103 and induces apoptosis. Biochem Biophys Res Commun 336:876–881
10. **Nishi Y, Yanase T, Mu Y, Oba K, Ichino I, Saito M, Nomura M, Mukasa C, Okabe T, Goto K, Takayanagi R, Kashimura Y, Haji M, Nawata H** 2001 Establishment and characterization of a steroidogenic human granulosa-like tumor cell line, KGN, that expresses functional follicle-stimulating hormone receptor. Endocrinology 142:437–445
11. **Beysen D, Moumné L, Veitia R, Peters H, Leroy BP, De Paepe A, De Baere E** 2008 Missense mutations in the forkhead domain of FOXL2 lead to subcellular mislocalization, protein aggregation and impaired transactivation. Hum Mol Genet 17:2030–2038
12. **Gurates B, Amsterdam A, Tamura M, Yang S, Zhou J, Fang Z, Amin S, Sebastian S, Bulun SE** 2003 WT1 and DAX-1 regulate SF-1-mediated human P450arom gene expression in gonadal cells. Mol Cell Endocrinol 208:61–75
13. **Michael MD, Kilgore MW, Morohashi K, Simpson ER** 1995 Ad4BP/SF-1 regulates cyclic AMP-induced transcription from the proximal promoter (PII) of the human aromatase P450 (CYP19) gene in the ovary. J Biol Chem 270:13561–13566
14. **Pannetier M, Fabre S, Batista F, Kocer A, Renault L, Jolivet G, Mandon-Pépin B, Cotinot C, Veitia R, Pailhoux E** 2006 FOXL2 activates P450 aromatase gene transcription: towards a better characterization of the early steps of mammalian ovarian development. J Mol Endocrinol 36:399–413
15. **Zhang P, Mellon SH** 1996 The orphan nuclear receptor steroidogenic factor-1 regulates the cyclic adenosine 3′,5′-monophosphate-mediated transcriptional activation of rat cytochrome P450c17 (17α-hydroxylase/c17-20 lyase). Mol Endocrinol 10:147–158
16. **Jeyasuria P, Ikeda Y, Jamin SP, Zhao L, De Rooij DG, Themmen AP, Behringer RR, Parker KL** 2004 Cell-specific knockout of steroidogenic factor 1 reveals its essential roles in gonadal function. Mol Endocrinol 18:1610–1619
17. **Zhou LY, Wang DS, Shibata Y, Paul-Prasanth B, Suzuki A, Nagahama Y** 2007 Characterization, expression and transcriptional regulation of P450c17-I and -II in the medaka, *Oryzias latipes*. Biochem Biophys Res Commun 362:619–625
18. **De Baere E, Beysen D, Oley C, Lorenz B, Cocquet J, De Sutter P, Devriendt K, Dixon M, Fellous M, Fryns JP, Garza A, Jonsrud C, Koivisto PA, Krause A, Leroy BP, Meire F, Plomp A, Van Maldergem L, De Paepe A, Veitia R, Messiaen L** 2003 FOXL2 and BPES: mutational hotspots, phenotypic variability, and revision of the genotype-phenotype correlation. Am J Hum Genet 72:478–487
19. **Simpson JL** 2008 Genetic and phenotypic heterogeneity in ovarian failure: overview of selected candidate genes. Ann NY Acad Sci 1135:146–154
20. **Santoro N** 2001 Research on the mechanisms of premature ovarian failure. J Soc Gynecol Investig 8:S10–S12
21. **Jagarlamudi K, Reddy P, Adhikari D, Liu K** 2010 Genetically modified mouse models for premature ovarian failure (POF). Mol Cell Endocrinol 315:1–10
22. **Matzuk MM, Lamb DJ** 2002 Genetic dissection of mammalian fertility pathways. Nat Cell Biol 4(Suppl):s41–s49
23. **Shapiro DB, Pappalardo A, White BA, Peluso JJ** 1996 Steroidogenic factor-1 as a positive regulator of rat granulosa cell differentiation and a negative regulator of mitosis. Endocrinology 137:1187–1195
24. **Suzuki T, Sasano H, Tamura M, Aoki H, Fukaya T, Yajima A, Nagura H, Mason JI** 1993 Temporal and spatial localization of steroidogenic enzymes in premenopausal human ovaries: in situ hybridization and immunohistochemical study. Mol Cell Endocrinol 97:135–143